Energy Flow (Bond Graph) Dynamic Modeling of Cartesian-Frame FFF 3-D Printer Gantry

Maharshi A. Sharma[1] and Albert E. Patterson[1,2]

[1]Department of Mechanical Engineering, Texas A&M University, College Station, TX 77843
[2]Manufacturing and Mechanical Engineering Technology, Department of Engineering Technology and Industrial Distribution,
Texas A&M University, College Station, TX, 77843

maharshiarindom@tamu.edu; aepatterson5@tamu.edu

Abstract

Energy flow (bond graph) modelling gives important information about the flow of energy to each component of a dynamic system and is especially useful for complex non-linear mechanical systems. This work presents a systematic development of a bond graph model of fused filament fabrication (FFF) 3D printer gantry. The model incorporates structural and belt stiffness, damping and input torque. The model was checked for correctness and causality using the 20-SIM software. The model was further validated using MATLAB-Simulink using parameters obtained for an example printer characterized in a lab environment. The bond graph model gives a unique view into modelling of the extruder carriage dynamics in FFF and can be applied to specific problems. It will also give interesting information on the controllability and system integration of the printer hardware.

Keywords: FFF process; extrusion-based additive manufacturing; bond-graph model; dynamic modeling

---

1. Introduction

One of the common and useful ways to model mechanical systems is via the bond graph method, where exchanges of energy are modeled to simulate the behavior of the system. The method is discussed in depth in [1-4]. Bond graphs can also be used to generate algorithms to monitor operations in industries [5]. It provides a way of pictorial representation of the entire system consisting of multiple disciplines [6].
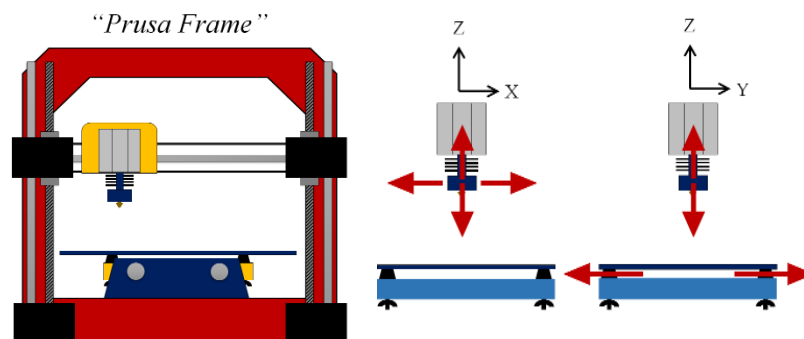

Figure 1: Prusa frame printer system [16]. Adapted per the terms of a CC-BY license.

One of the most common additive manufacturing processes is the fused filament fabrication (FFF) process, which uses a heated nozzle to selectively extrude thermoplastic feedstock to build parts up in layers. This is typically done using a cartesian-based 3-axis system. The basic machine has two major components moving relative to each

other, the extruder head, and the build plate, within the x-y-z coordinate system [7-10]. This current research focusses on Prusa-frame printers where the extruder carriage moves in X axis and Z axis direction and the build plate moves in Y axis direction. Figure 1 shows the representative diagram basic Prusa-frame printer system and its axes of motion in coordinate system. This design allows the fastest printing speed of any of the cartesian-frame printers, is the easiest to use with thin layers (50-100μm) and has the lowest sensitivity to filament quality [11]. A clear understanding of the different types is essential in the correct modeling of the system to be applicable for modeling the extruder carriage motion.

Bond graph presents an effort and flow representation of the system depicting the flow of energy from one component to another. The **0** in the bond graph are common effort (Force) and **1** are the common flow (velocity) junctions. **0** junction is generally used for velocity distribution and **1** junction is used for energy distribution. The half arrow indicates the positive and negative directions of flow. **I** represent inertia; **R** represents resistance, in this study it represents damping; **C** represents compliance or 1/k. **TF** represents transformer, in this study it represents a ratio to be multiplied along the flow; and **SE** represents effort, for the purpose of this study it represents the external force applied.

2. System Model Development
2.1 Printer Model

The FFF system has three major components [7-10], the frame, the extruder carriage, and the build plate. For the purposes of the present study, the motion of the build plate is neglected and assumed to be static relative to the extruder head. The plant for the rest of the printer can be divided into three major systems, each with a compliant connection; these are the (1) frame support structure (desk or workbench), (2) the printer frame, and (3) the extruder motion system.
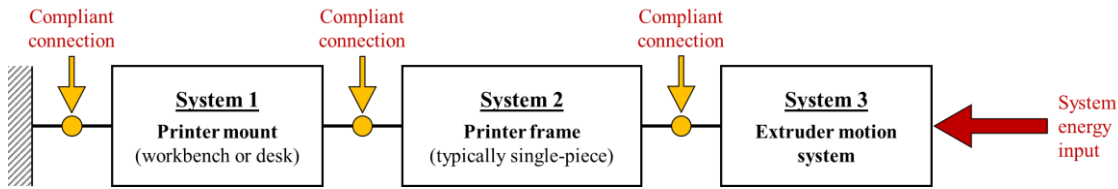

Figure 2: FFF machine plant configuration

The mount is connected to the system ground, while the energy input for the system flows into the extruder system. The energy for extruder carriage motions comes from motors mounted within the extruder motion system. These motors drive the mechanical components and induce the vibrations into the rest of the system. After further development of the system model shown in Figure 2, the spring-mass-damper model of the plant used in the extruder carriage motion can be derived (Figure 3) in x-z coordinates. The definitions for each of the variables and parameters are shown in Table 1.
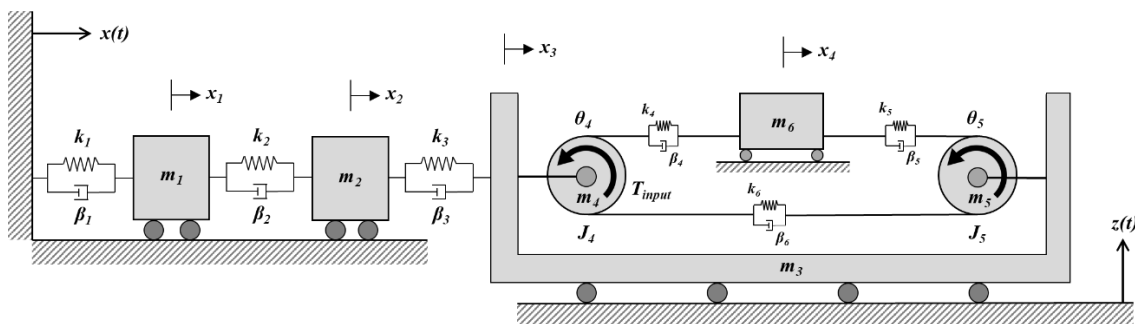

Figure 3: Extruder carriage dynamic model

Table 1: Extruder carriage dynamic model parameters

State Variable		Parameter	
x_1	Position of printer mount (m)	k_1	Stiffness between ground and mount (N/m)
x_2	Position of frame (m)	k_2	Stiffness between mount and frame (N/m)
x_3	Position of extruder motion system (m)	k_3	Stiffness between frame and carriage motion system (N/m)
x_4	Position of extruder carriage (m)	k_4	Stiffness of belt section 1 (N/m)
θ_4	Angular position of Pulley 4 $(radians)$	k_5	Stiffness of belt section 2 (N/m)
θ_5	Angular position of Pulley 5 $(radians)$	k_6	Stiffness of belt section 3 (N/m)
Parameter		β_1	Energy dissipation between ground and mount $(N.s/m)$
m_1	Mass of printer mount (kg)	β_2	Energy dissipation between mount and frame $(N.s/m)$
m_2	Mass of printer frame (kg)	β_3	Energy dissipation between frame and motion $(N.s/m)$
m_3	Mass of extruder motion system frame (kg)	β_4	Energy dissipation in belt section 1 $(N.s/m)$
m_4	Mass of Pulley 4 (kg)	β_5	Energy dissipation in belt section 2 $(N.s/m)$
m_5	Mass of Pulley 5 (kg)	β_6	Energy dissipation in belt section 3 $(N.s/m)$
m_6	Mass of extruder carriage (kg)	$z(t)$	Extruder carriage height (mm)

The equations of motion for this dynamic system are derived using Newton-Euler method. Eqs 1-6 below describe the equations of motion for the FFF Printer system shown in Figure 3.

$$\ddot{x}_1 = -\frac{k_1 + k_2}{m_1}x_1 + \frac{k_2}{m_1}x_2 - \frac{\beta_1 + \beta_2}{m_1}\dot{x}_1 + \frac{\beta_2}{m_1}\dot{x}_2 \tag{1}$$

$$\ddot{x}_2 = \frac{k_2}{m_2}x_1 - \frac{k_2 + k_3}{m_2}x_2 + \frac{k_3}{m_2}x_3 + \frac{\beta_2}{m_2}\dot{x}_1 - \frac{\beta_2 + \beta_3}{m_2}\dot{x}_2 + \frac{\beta_3}{m_2}\dot{x}_3 \tag{2}$$

$$\ddot{x}_3 = \frac{k_3}{m_{3t}}x_2 - \frac{(k_3 + k_4 + k_5)}{m_{3t}}x_3 + \frac{(k_4 + k_5)}{m_{3t}}x_4 + \frac{k_4 R}{m_{3t}}\theta_4 + \frac{k_5 R}{m_{3t}}\theta_5 + \frac{\beta_3}{m_{3t}}\dot{x}_2$$
$$- \frac{(\beta_3 + \beta_4 + \beta_5)}{m_{3t}}\dot{x}_3 + \frac{(\beta_4 + \beta_5)}{m_{3t}}\dot{x}_4 + \frac{\beta_4 R}{m_{3t}}\dot{\theta}_4 + \frac{\beta_5 R}{m_{3t}}\dot{\theta}_5 \tag{3}$$

$$\ddot{x}_4 = \frac{(k_4 + k_5)}{m_6}x_3 - \frac{(k_4 + k_5)}{m_6}x_4 - \frac{R k_5}{m_6}\theta_5 - \frac{R k_4}{m_6}\theta_4 + \frac{(\beta_4 + \beta_5)}{m_6}\dot{x}_3$$
$$- \frac{\beta_4 + \beta_5}{m_6}\dot{x}_4 - \frac{\beta_4 R}{m_6}\dot{\theta}_4 - \frac{\beta_5 R}{m_6}\dot{\theta}_5 \tag{4}$$

$$\ddot{\theta}_4 = -\frac{2k_4}{m_4 R}x_4 + \frac{2k_4}{m_4 R}x_3 + \frac{2(k_4 + k_6)}{m_4}\theta_4 + \frac{2k_6}{m_4}\theta_5 + \frac{2\beta_4}{m_4 R}\dot{x}_3 - \frac{2\beta_4}{m_4 R}\dot{x}_4$$
$$- \frac{2(\beta_4 + \beta_6)}{m_4}\dot{\theta}_4 + \frac{2\beta_6}{m_4}\dot{\theta}_5 + \frac{2T_{input}}{m_4 R^2} \tag{5}$$

$$\ddot{\theta}_5 = \frac{2k_5}{m_5 R}x_3 - \frac{2k_5}{m_5 R}x_4 - \frac{2(k_5 + k_6)}{m_5}\theta_5 + \frac{2k_6}{m_5}\theta_4 + \frac{2\beta_5}{m_5 R}\dot{x}_3$$
$$- \frac{2\beta_5}{m_5 R}\dot{x}_4 + \frac{2\beta_6}{m_5}\dot{\theta}_4 - \frac{2(\beta_5 + \beta_6)}{m_5}\dot{\theta}_5 \tag{6}$$

2.2. Bond-Graph Model

The bond-graph model of the system is developed systematically to provide a better understanding of the sub-system and the flow of energy through the components. The printer system has been divided into system level blocks as shown in Figure 1 and into isolated extruder system, which when added gives the printer configuration.

The bond graph model in Figure 4 shows how the force applied at block m_3 is transmitted throughout the system. The spring and damper system between blocks m_1 and m_2 and between blocks m_2 and m_3 acts on relative velocity between these blocks. The velocity is divided using the **0** junction while **1** junction represents the common velocity points connecting the springs and dampers of same relative velocity. The **1** junction also connects the masses and is used to analyze the velocity of these masses.
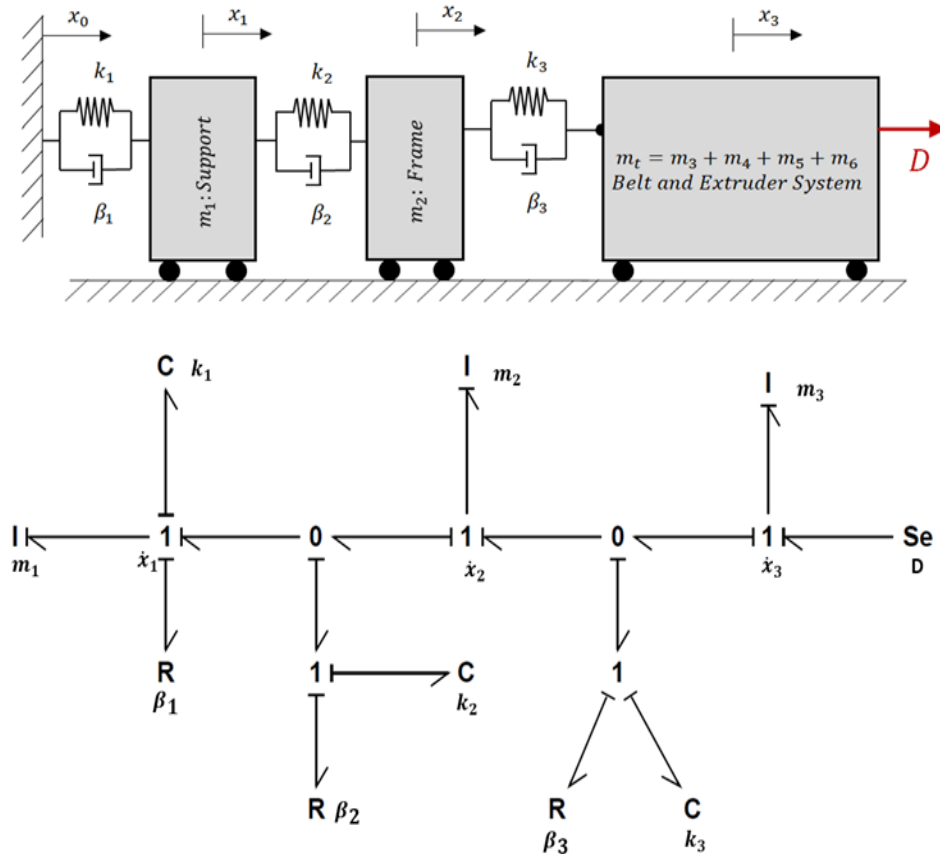

Figure 4: Printer block system (above) and bond graph model of the system (below)

Figure 4, 5 and 6 shows a series of simplified mechanical systems that, when combined, constitute the mechanical system of the FFF extruder carriage (similarly to the method discussed in the Newton-Euler model derivation); note that D is the generic connection force between the systems when they are connected during use. The most basic component is the simple drive belt system with two equally sized and equally massed pulleys and no slippage, shown in Figure 5a. The drive belt system is similar to the gantry system without the printer head. It is assumed that $T_1 > T_2$, which will be important in assigning directions in the bond graph model. Figure 5b and 5c represent the bond graph model of the pulley system. Both these bond graphs represent the same system, giving the same results. The bond graph in Figure 5b is derived using efforts approach showing a step-by-step flow of energy or force throughout the system. Figure 5c is derived using the flow approach depicting the division of velocities at various junctions in the system.
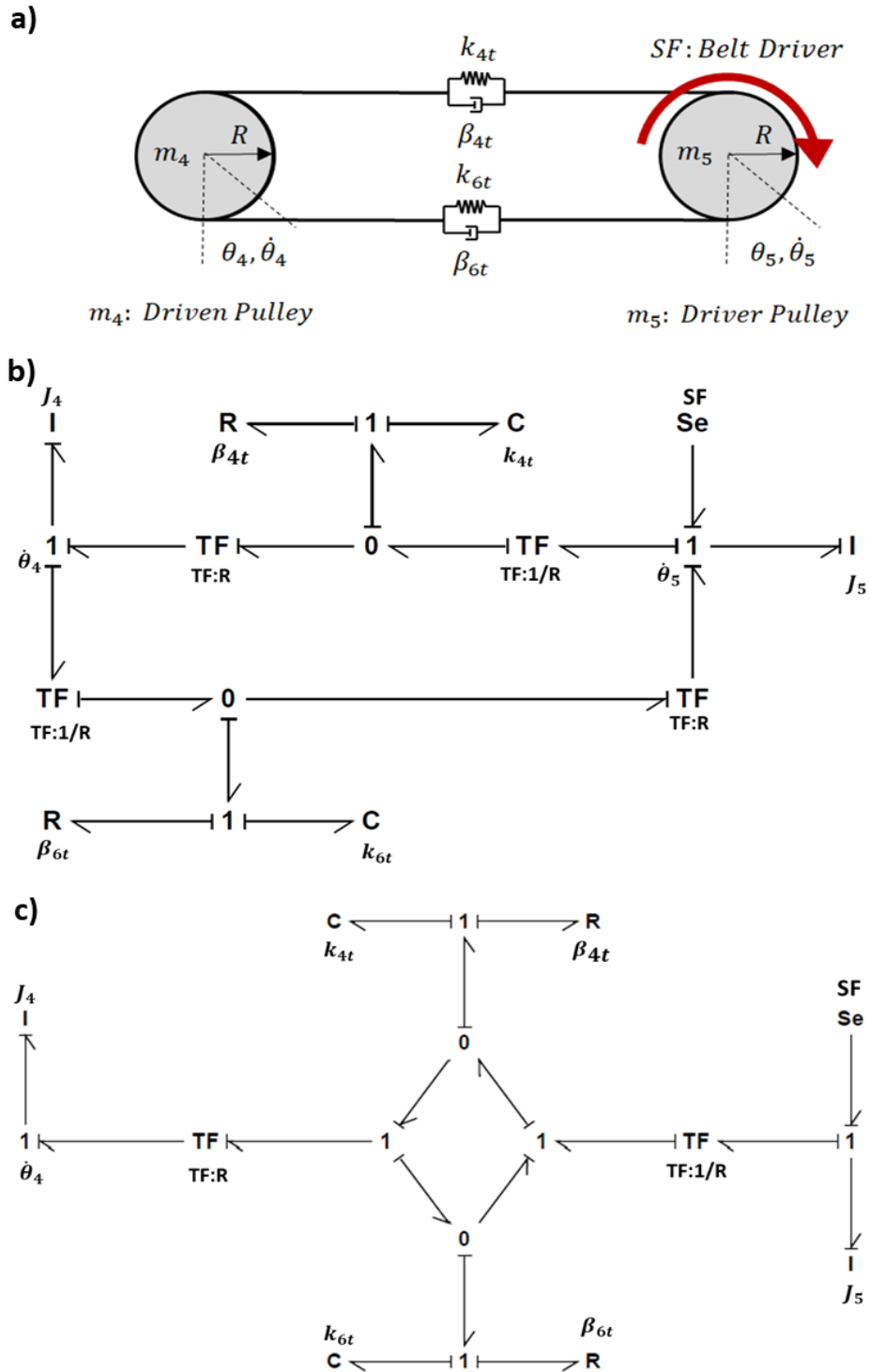
Figure 5: a) Drive belt system, b) bond graph of the system using efforts approach, c) bond graph model of the system using flow approach
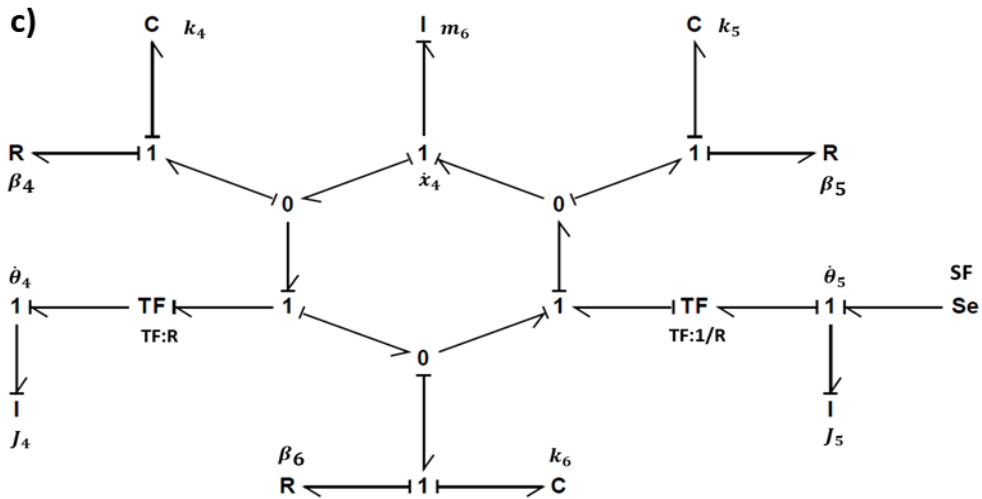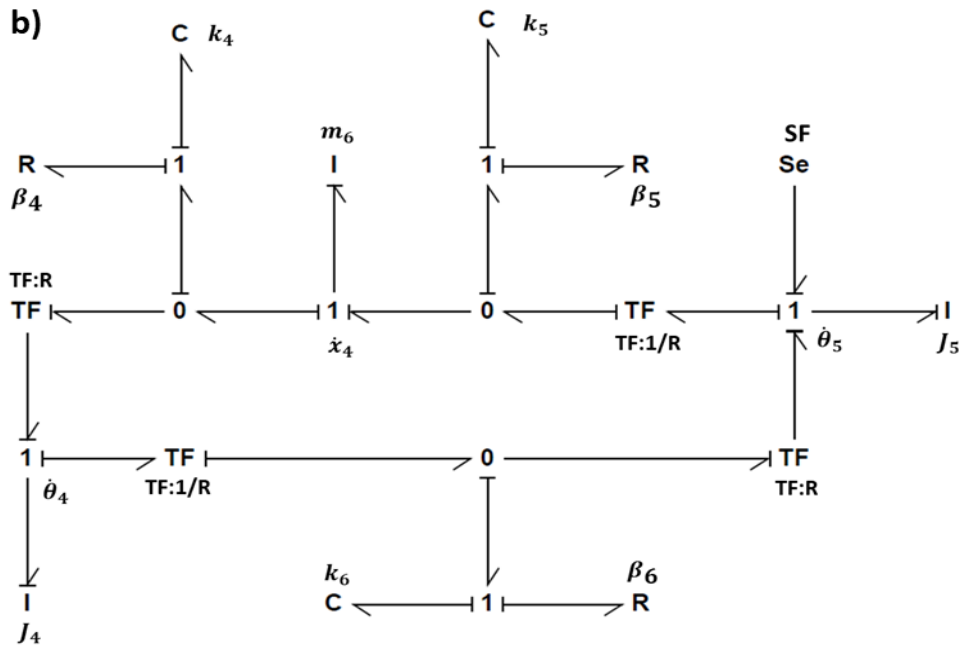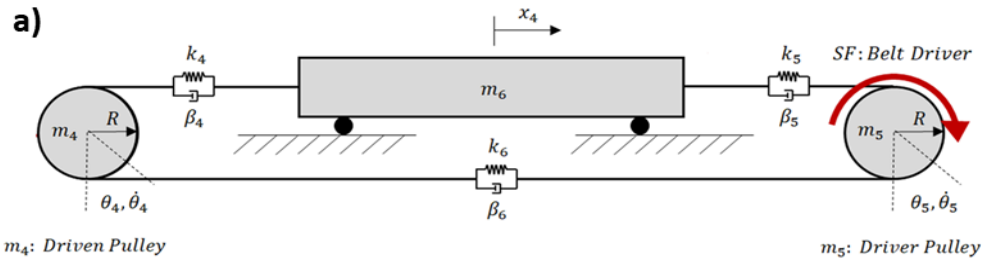
Figure 6: a) Extruder system, b) bond graph of the system using efforts approach, c) bond graph model of the system using flow approach

If Figure 5a is modified to include a carriage, the result of the model will be Figure 6a representing the model of extruder carriage system. Figures 6b and 6c represent the bond graph model of the extruder carriage system. The bond graph in Figure 6b is derived using efforts approach similar to figure 5b; Figure 6c is derived using the flow approach similar to Figure 5c.
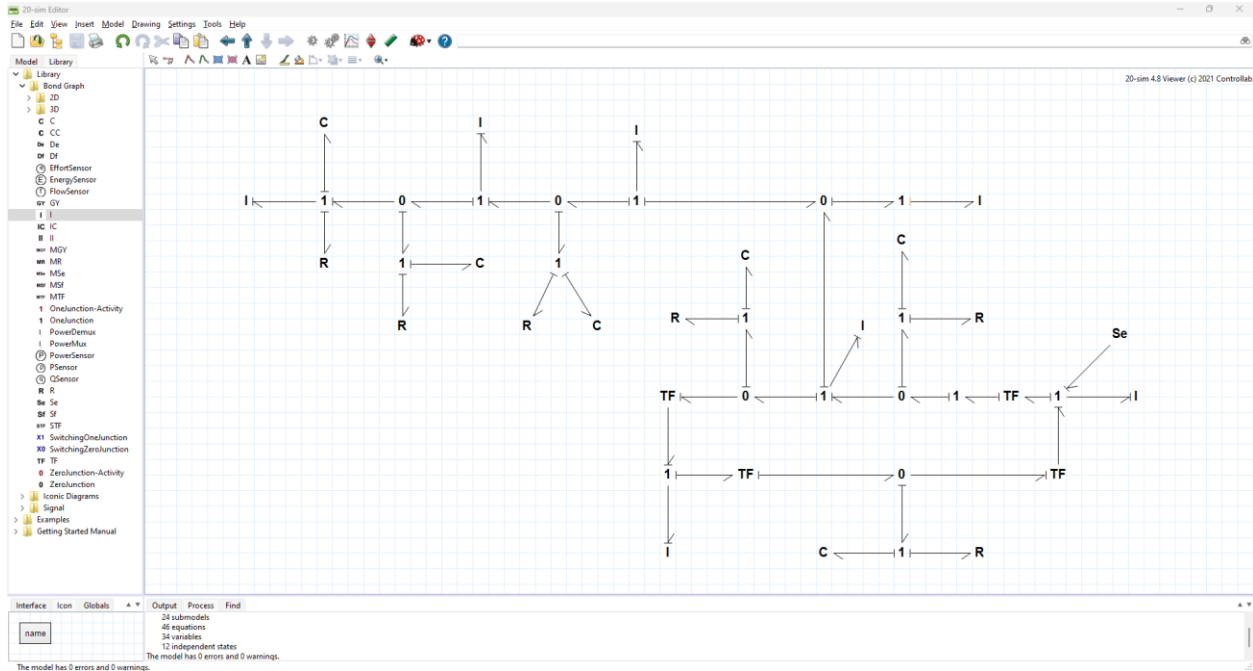
Combining the bond graph of these sub-systems in Figure 5 and 6 provides the bond graph of the entire 3D printer (Figure 7). The dashed rectangular box in the bond graph in Figure 7 is similar to the bond graph shown in Figure 4. The flow method approach can be easily derived and is not shown here, although it is very similar to combining the bond graphs in Figures 4 and 6, while following the causality notation in the intersection shown in Figure 7. The torque applied into the system is through the pulley inside block m_3, thus rotating the pulley which in turn moves the carriage. Applying Newton's Law into the system, it can be observed that the block m_3 will move in the opposite direction of the carriage. Hence the flow and causality notation direction in the intersection between the extruder carriage system and the block system is clearly represented. This bond graph (Figure 7) can be used to measure both absolute and relative velocity of the extruder carriage system when it is in motion. The causality directions and bonds must be carefully considered and numbered in order to show the correct way to analyze or simulate the system using this method.

Figure 7: 3D printer system (above) and the bond graph of the entire 3D printer system

Figure 8: Screenshot of the full system bond-graph model in 20-SIM

One of the features of bond graph models is the ability to directly produce the equations of motion for the system or its state space equations [6]. However, this exercise can be very impractical for large systems such as the one presented here, and the bond graph is better used directly in simulation of the system [1] using one of the many tools available for this purpose. The purpose of the developing this bond graph model is to give an additional view into the modeling of the extruder carriage dynamics in FFF and to provide an additional tool which can be applied (or modified as needed) to specific problems. All the models presented were carefully checked for correctness and proper causality using the 20-SIM® tool (University of Twente, Enschede, Netherlands), using simple inputs to ensure it behaved as expected. Figure 8 shows a screenshot of the bond-graph model in *20-SIM*.

3. System Simulation

The bond graph model of the sub-systems and the complete system have been shown in Figures 4-7. While bond graphs can accommodate variable stiffness in the models, for the sake of this study, it was assumed that the stiffness and damping coefficient of the system were constant. The causality of the bond graphs was already verified using *20-SIM* software in deriving the models. The equations of motion of the sub-systems and the complete systems shown were derived using Newton-Euler method to construct a MATLAB-Simulink model. The Simulink models for the bond graph systems are shown in the Appendix. The motion of the systems in the bond graph model were compared with the motion of the dynamic model in Simulink to validate the bond graphs. Note that arbitrary values of the parameters not related to this study were used to compare the results. Figure 9 shows the velocity of each block of the block system shown in Figure 4. Figure 10 represents the velocity of the pulleys and the carriage of the extruder system mentioned in the bond graph in Figure 6. The velocity plot of the complete 3D printer system is shown in Figure 11 and its corresponding bond graph is mentioned in Figure 7. In Figure 11 only the velocity of m3 block and extruder carriage is shown to verify the link between the sub systems. The plot in Figures 9-11 is obtained through bond graph using *20-SIM* and the bottom plot is obtained through equation of motion of the system using *Simulink*. It can be clearly seen that both these methods produced the same results for the block system, extruder system and the complete 3D printer system.
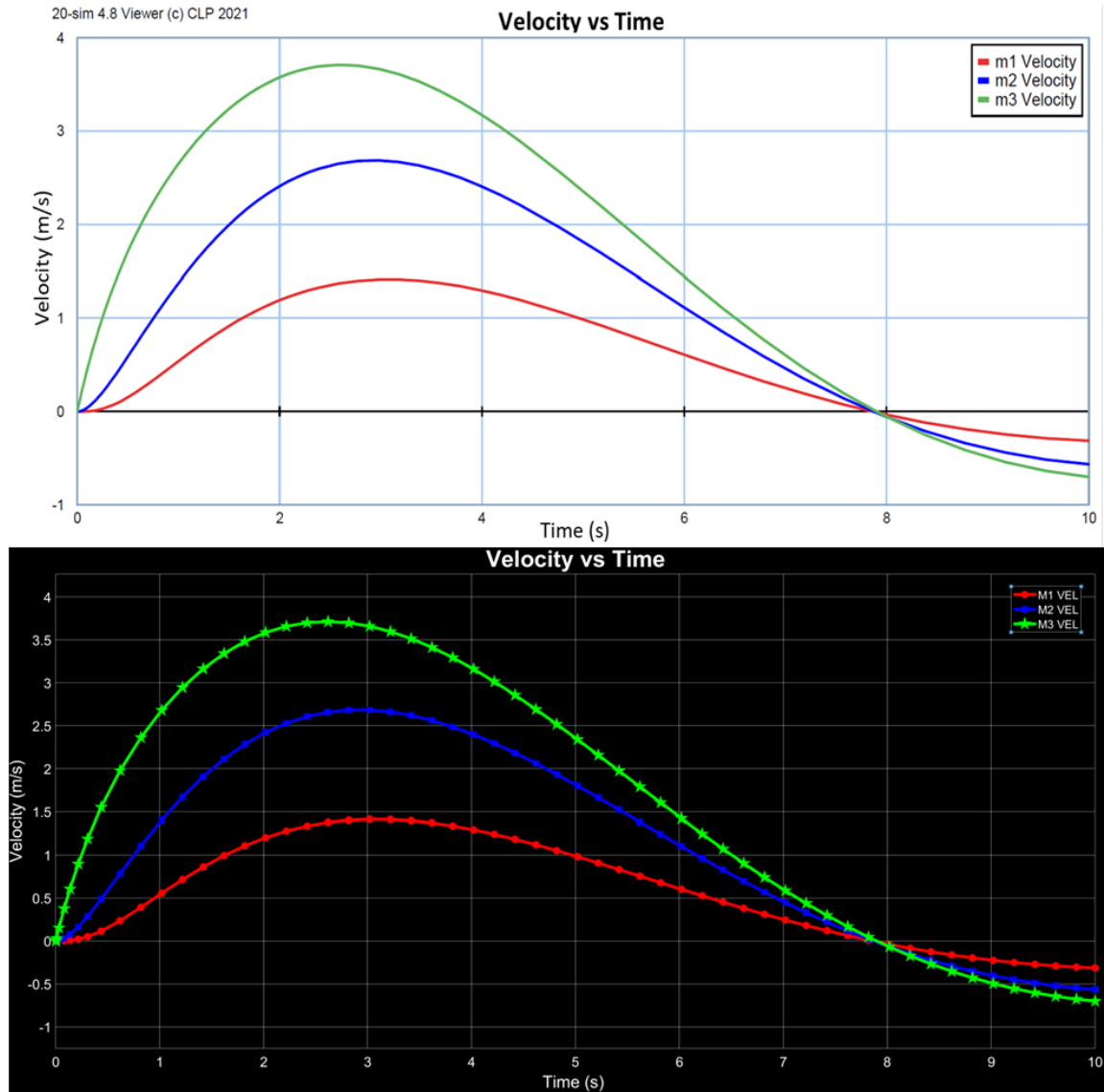
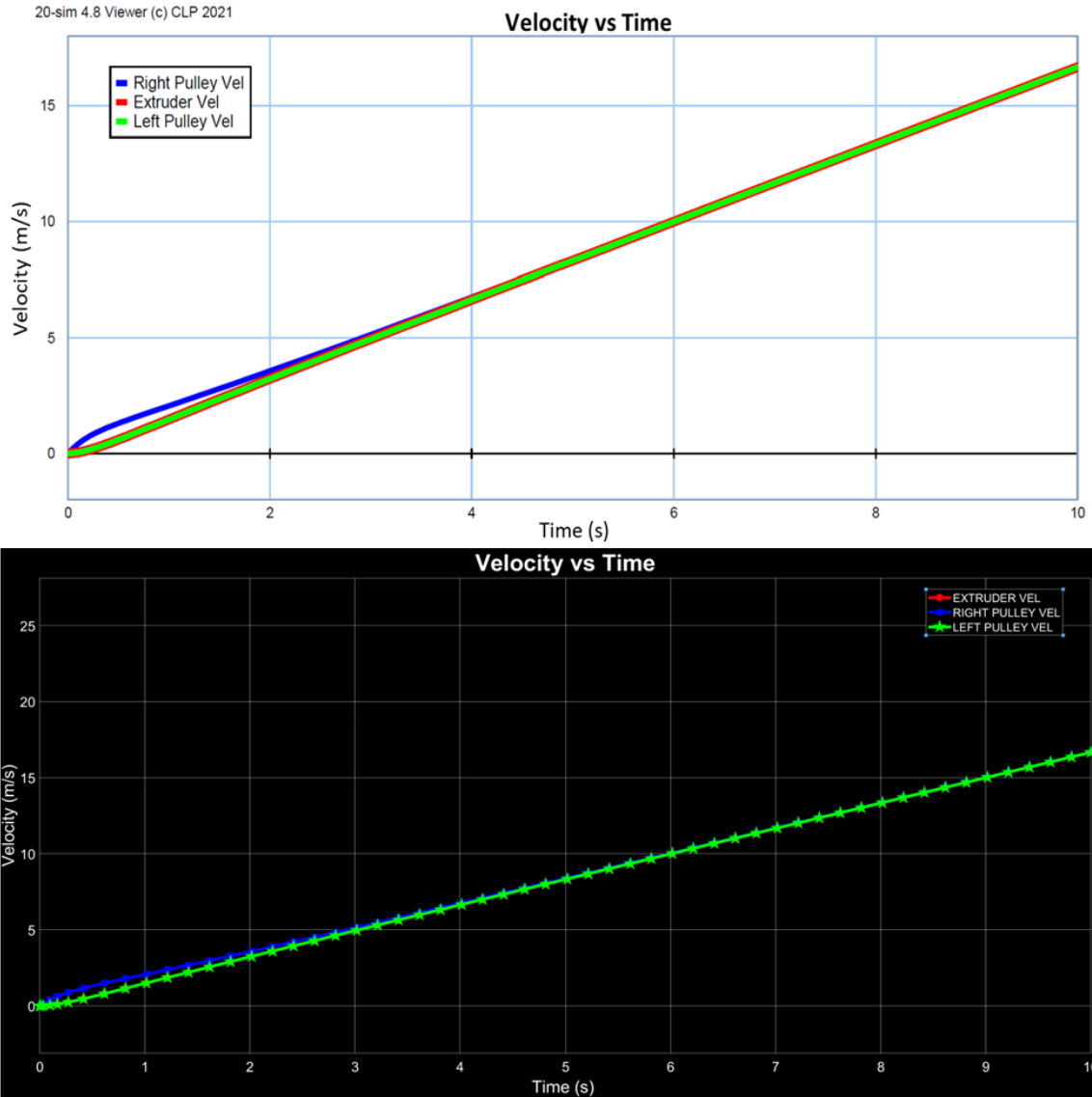**Figure 9:** Velocity vs time plot of the block system obtained in 20-SIM (above) and Simulink (below)

Figure 10: Velocity vs time plot of the extruder system obtained in 20-SIM (above) and Simulink (below)
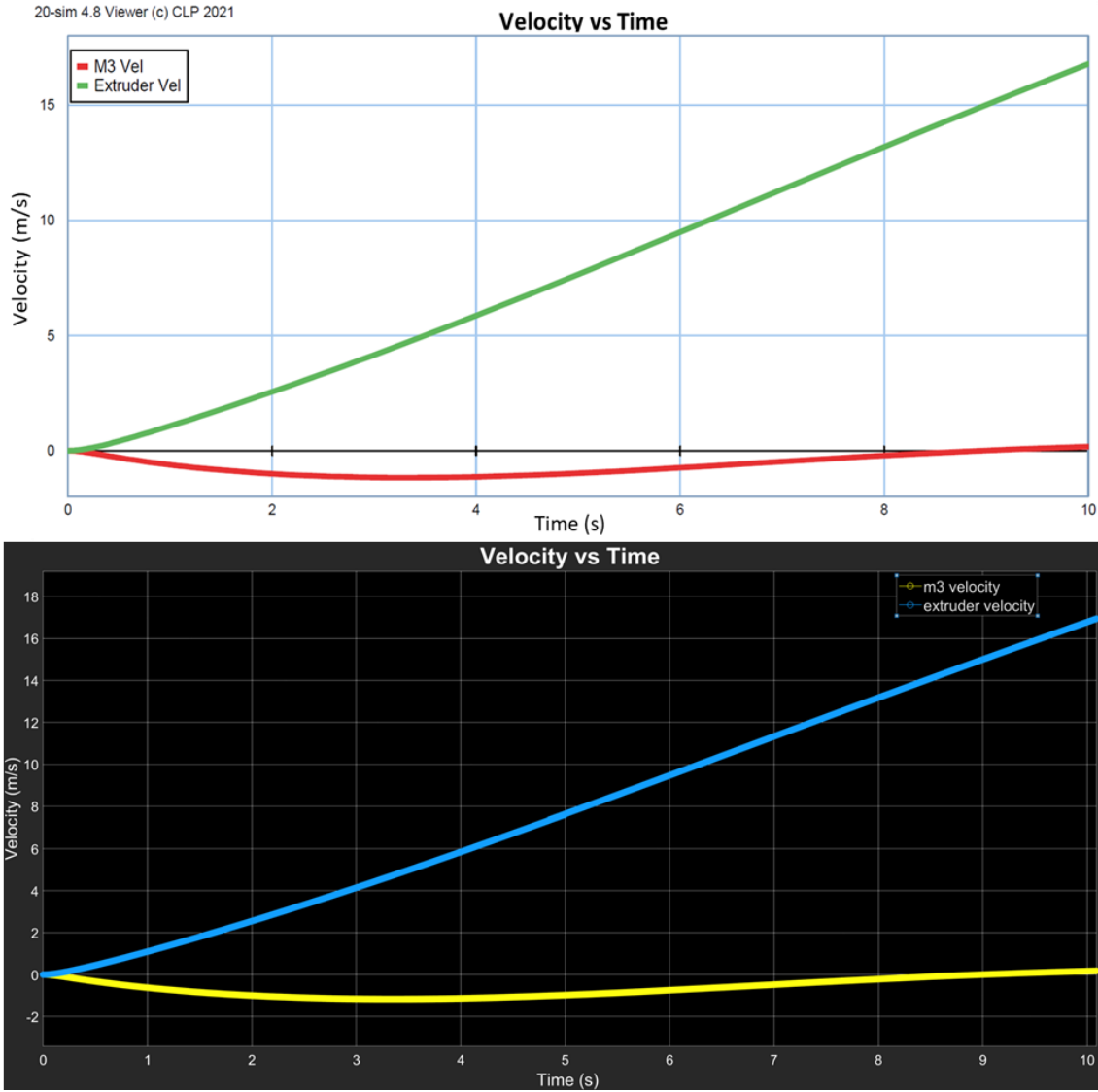
Figure 11: Velocity vs time plot of the 3D printer system obtained in 20-SIM (above) and Simulink (below)

4. Conclusions and Future Work

The Bond-graph model presented here provides a different insight into the system with interesting information of the hardware integration through its energy flow model. The bond-graph model developed represents the 3D printer in study accurately and can be used to track the extruder gantry motion. The bond graph model developed can be used to represent a prusa-frame cartesian coordinate FFF 3D printer in complex industrial systems as well as to study the motion and flow within the system. The advantage of bond-graphs is that they can be extended to incorporate electro-mechanical systems and non-linear systems for a comprehensive study of dynamic systems. Bond-graph model can be further developed to incorporate non-linear parameters as well as motion in all 3 dimensions.

Acknowledgements

Raw Data and Code

All raw data and code for this work are available upon request to the authors.

References

1. Banerjee, N., Saha, A.K., Karmakar, R., & Bhattacharyya, R. (2009). Bond graph modeling of a railway truck on a curved track. *Simulation Modelling Practice and Theory, 17*: 22-34.
2. Borutsky, W. (1999). Bond graph modeling from an object oriented modeling point of view. *Simulation Practice and Theory, 7*: 439-461.
3. Toloni, A., Amati, N., & Zenerino, E. (2006). Dynamic Modeling of belt Drive Systems: Effects of Shear Deformations. *Journal of Vibrations and Acoustics, 128*: 555-567.
4. Sanchez, R. & Medina, A. (2014). Wind turbine model simulation: A bond graph approach. *Simulation Modelling Theory and Practice, 41*: 28-45.
5. Samantaray, A.K. and Bouamama, B.O., 2008. Model-based process supervision: a bond graph approach. London: Springer.
6. Borutzky, W., (2011). Bond graph modelling of engineering systems (Vol. 103). New York: Springer.
7. Crump, S.S. (1992). *US Patent 5,121,329* "Apparatus and method for creating three-dimensional objects". Washington, DC: US Patent Office.
8. Masood, S.H. (1996). Intelligent rapid prototyping with fused deposition modelling. *Rapid Prototyping Journal, 2*(1): 24-33.
9. Turner, B.N., Strong, R., & Gold, S.A. (2014). A review of melt extrusion additive manufacturing processes: I. Process design and modeling. *Rapid Prototyping Journal, 20*(3): 192-204.
10. Messimer, S.L., Patterson, A.E., Muna, N., et al (2018). Characterization and Processing Behavior of Heated Aluminum-Polycarbonate Composite Build Plated for the FDM additive Manufacturing Process.
11. Patterson, A. E., Chadha, C., and Jasiuk, I. M., 2021, "Identification and Mapping of Manufacturability Constraints for Extrusion-based Additive Manufacturing", Journal of Manufacturing and Materials Processing, 5(2), p. 33.

Appendix

1. Simulink Model for the Bond-Graphs

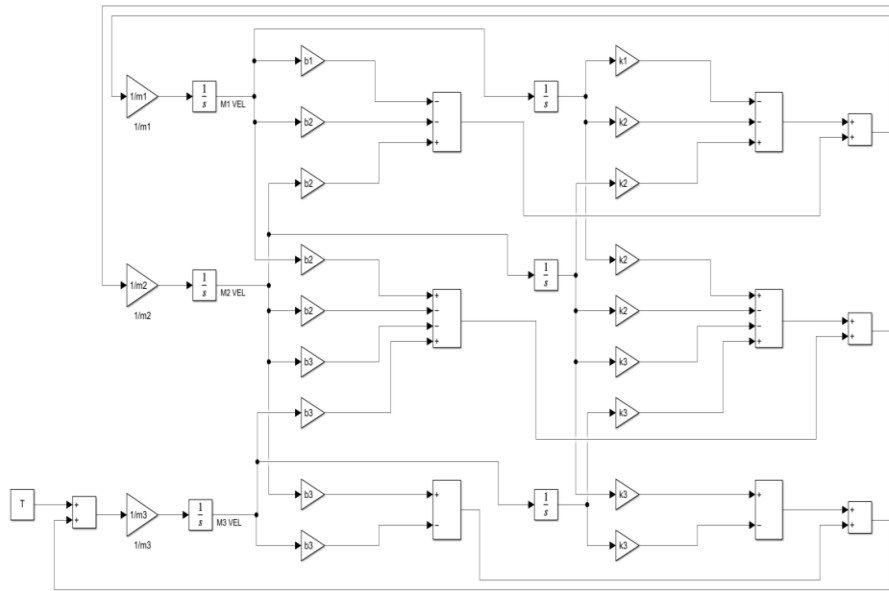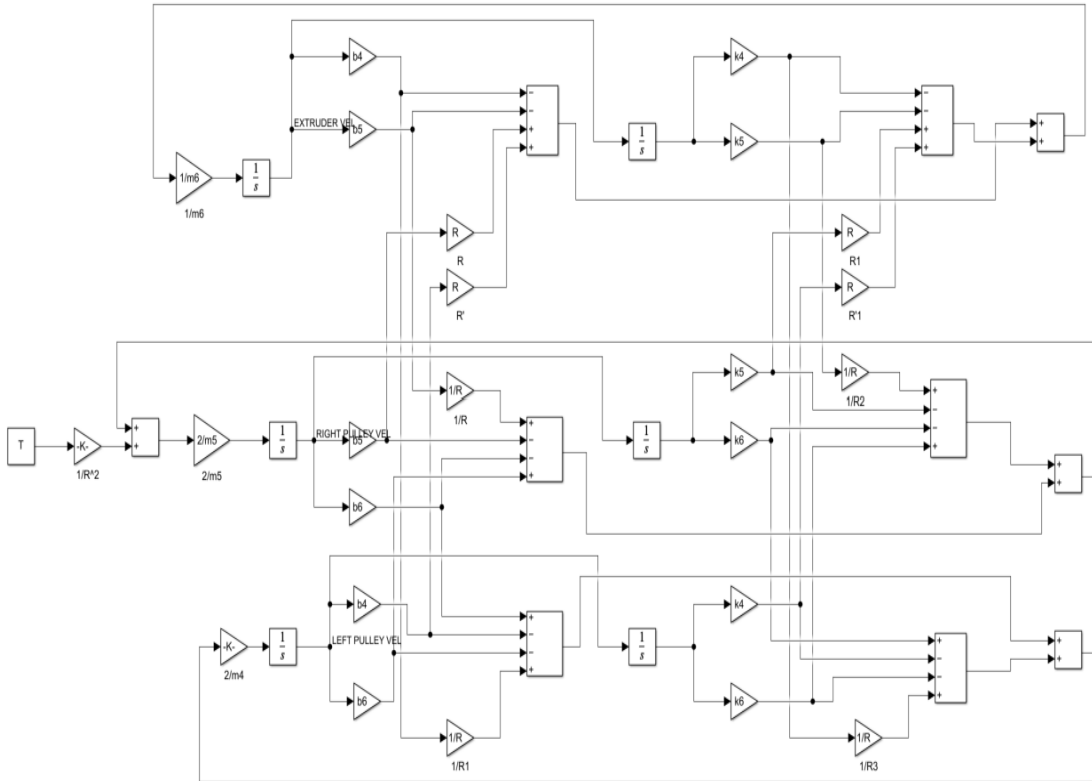**Figure 12:** Simulink model for block system
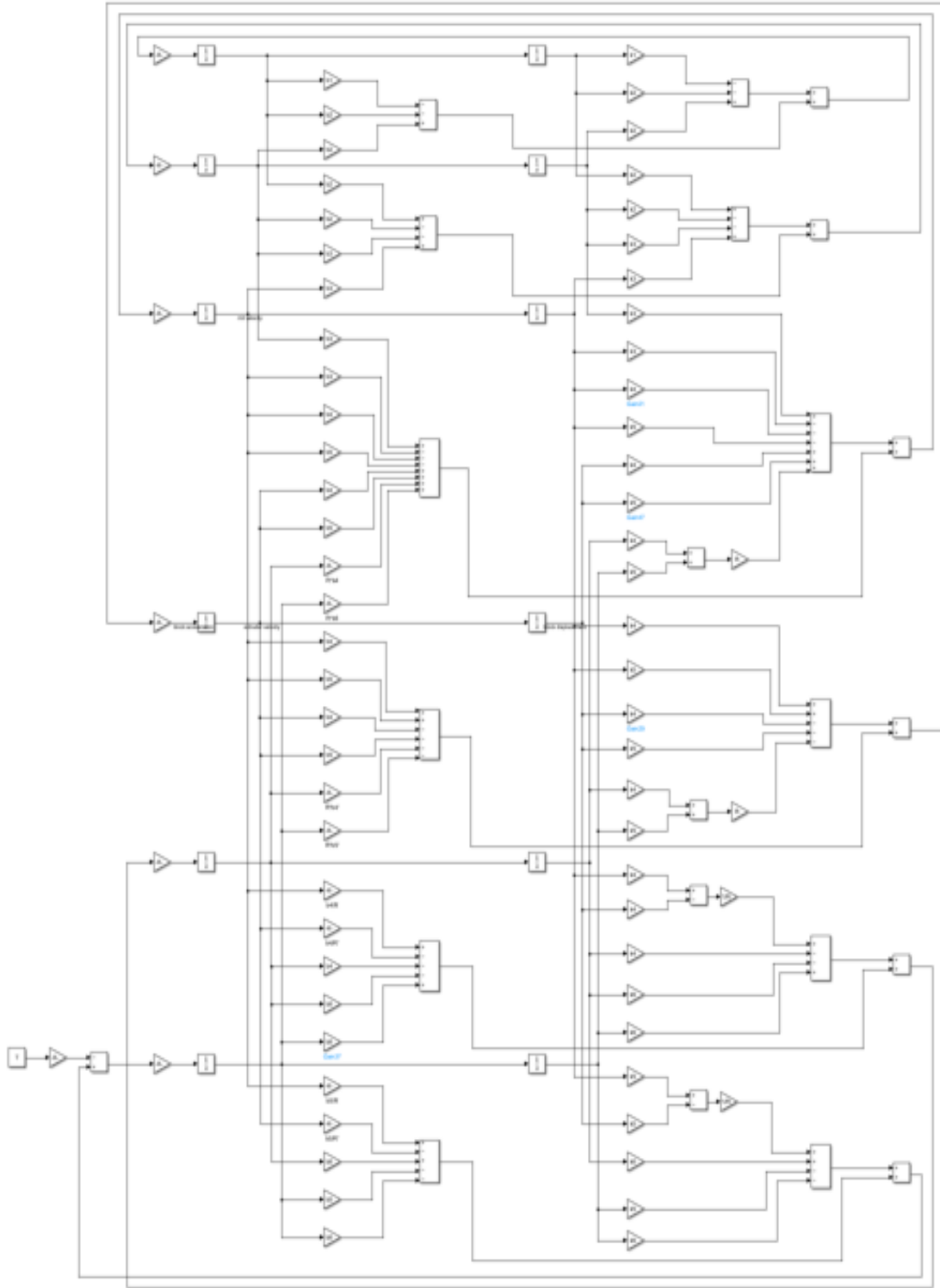

Figure 13: Simulink model for the extruder system

Figure 14: Simulink model for the complete printer system